

Effects of the pseudo-gap on the field-induced kinetic energy density of $\text{Bi}_2\text{Sr}_2\text{CaCu}_2\text{O}_{8+\delta}$ single crystals

L. F. Lopes¹, J. P. Peña¹, M. A. Tumelero¹, J. Schaf¹, V. N. Vieira², P. Pureur¹

August 26, 2020

¹Instituto de Física, Universidade Federal do Rio Grande do Sul, ZIP 91501-970 Porto Alegre, RS, Brazil

²Instituto de Física e Matemática, Universidade Federal de Pelotas, ZIP 96010-900 Pelotas, RS, Brazil

Abstract

We report on magnetization experiments from which we obtain the field-induced kinetic energy density, E_k , in the superconducting phase of several $\text{Bi}_2\text{Sr}_2\text{CaCu}_2\text{O}_{8+\delta}$ single crystal samples. The kinetic energy magnitude changes according to the characteristic reduction of the single-electron density of states produced by the pseudogap in the underdoped limit. Moreover, a remarkable peak of E_k occurring at the specific holes density $p \sim 0.18$ is related to a van Hove singularity due to the pseudogap closure. We also extracted the superfluid density, ρ_s . We conclude that E_k and ρ_s are related to the pseudogap energy scale. This result is understood as an evidence of the coexistence between superconductivity and the pseudogap phenomenon in the $\text{Bi}_2\text{Sr}_2\text{CaCu}_2\text{O}_{8+\delta}$ cuprate compound.

Keywords: pseudogap, vortices-kinetic-energy-density, superconducting vortex dynamics

1 Introduction

The pseudogap phenomenon has been a longstanding subject in the physics of the high temperature superconducting cuprates (HTSC). This property is characterized by a sharp depression of the single-electron density of states (DOS) at the Fermi level and manifests more vigorously in the underdoped specimens. Moreover, the pseudogap problem has been shown to be closely related to the interplay between superconductivity and spin or charge degrees of freedom. Experimentally, the pseudogap effects arise below a characteristic temperature T^* , also known as the pseudogap temperature. For the most severely underdoped samples T^* is sensibly higher than the superconducting critical temperature T_c ; thus, the experimental manifestations of the pseudogap in photoelectron spectroscopy [1, 2], specific heat [3, 4], nuclear magnetic resonance (NMR) [5], tunneling conductance [6], transport [7] and optical properties [8] of the HTSC, are commonly observed in their normal phase (see Ref. [9] for an extended review on the pseudogap).

Although the presence of the pseudogap has been widely reported in several HTSC, a complete physical description of this phenomenon is still missing. Experimentally, the fact that the region where the pseudogap is observed extends mainly into the underdoped part of the temperature vs. holes concentration phase diagram has been reported as an universal characteristic of the HTSC [10]. It is not clear, nonetheless, whether the $T^*(p)$ curve represents a true phase transition boundary delimiting a pseudogap phase, or if it only identifies a crossover line occurring in a more or less broad temperature interval. In the underdoped part of the T vs. p diagram, where $T^* > T_c$, the doping dependence of T^* is fairly well known [11, 12]. On the other hand, the evolution of the T vs. p line across the optimal and overdoped regions is a matter of controversy.

In the last 30 year's numerous theories to describe the pseudogap have been proposed, most of them converging to one of three different scenarios. In the first one, also known as phase-fluctuation scenario (or preformed pairs scenario), the pseudogap is treated as a consequence of preformed incoherent electron pairs already present in temperatures higher than T_c [13]. In that case, the $T^*(p)$ -line should follow closely the superconducting dome in the overdoped region, vanishing together with superconductivity when the $T_c(p)$ -line reaches zero [1, 9]. A second scenario leads to interpretations where the pseudogap is attributed to excitations different from those related to superconductivity [11]; in this case the $T^*(p)$ -line should cut the superconducting dome ending in a quantum critical point (QCP) at some critical value p_{cp} , smaller than that defining the upper limit of the dome. A third and more recent scenario is also based on the competition between a charge or spin ordering phenomenon and superconductivity, but without the need of a QCP. These are the charge density wave, spin density wave [14, 15] and spin-charge separation [16, 17] scenarios.

All the above scenarios point to the same characteristics of the $T^*(p)$ -line in the normal phase of underdoped specimens. However, divergences arise when dealing with the superconducting phase and even with the normal phase of both under and overdoped samples [9]. Regarding the recently found experimental characteristics of the pseudogap in the normal phase, high precision torque-magnetometer experiments [18] and optical measurements [19] on $\text{YBa}_2\text{Cu}_3\text{O}_x$ (YBCO) samples detected evidences for broken rotational (nematic) and inversion (odd-parity magnetic phase) symmetry phases below T^* , respectively. Both of these results are in favor of the QCP scenario. Additionally, muon spin rotation measurements in YBCO led to the observation of slow magnetic fluctuations at temperatures close to T^* , indicating that the pseudogap is an authentic thermodynamic phase stabilized due to intra-cell spin ordering [20]. For the Bi-2212 system, a recent report using ultrahigh resolution resonant inelastic X-ray scattering showed evidence of dispersive charge density waves (CDW) closely related the pseudogap [21]. Notwithstanding the advances

made to detect and understand the trends of the pseudogap in the normal phase of the HTSC, the effects and consequences of this property inside the superconducting phase remain scarcely explored. Recent attempts to prove the interplay between the charge ordering and pseudogap effects in temperatures below T_c include the destruction of the superconducting state by using high magnetic fields [22, 23] and the employ of sophisticated techniques, as ultrasound spectroscopy [24].

Here we report on possible evidences of pseudogap effects in the superconducting phase of $\text{Bi}_2\text{Sr}_2\text{CaCu}_2\text{O}_{8+\delta}$ (Bi-2212) single crystals with different oxygen concentrations. We do this by analyzing the kinetic energy density (E_k) that is induced in the superconducting charge carriers of a type-II superconductor when it is submitted to a magnetic field in the vortex region of the phase diagram. Experimentally, this field-induced kinetic energy density may be obtained from the product of the equilibrium magnetization (\mathbf{M}) and the magnetic induction (\mathbf{B}) in the reversible region where no pinning effects are present. Mathematically, one writes [25]:

$$E_k = -\mathbf{M} \cdot \mathbf{B}. \quad (1)$$

Equation (1) is a consequence of the classical idea of the virial theorem applied to the Ginzburg-Landau (GL) theory [26]. Specifically, an spacial scale transformation is applied to the GL's free-energy where both the vector potential and the order parameter are transformed. By implementing boundary conditions for these two parameters, and by minimizing the energy with respect to the scale parameter, the expression $\mathbf{H} \cdot \mathbf{B} = 4\pi(E_k + 2E_f)$ (where E_k and E_f are the kinetic and magnetic-field energy densities, respectively) is obtained. This expression is the so called ‘‘Virial Theorem of Superconductivity’’ [26]. Finally, by expressing the magnetic induction in terms of \mathbf{H} and \mathbf{M} , and by utilizing a mean-field approximation for \mathbf{H} , the virial theorem can be re-arranged to yield E_k as seen in Eq. (1) [25]. This result represents the excess of kinetic energy density induced by an the external magnetic-field upon the superconducting pairs of an anisotropic Type-II superconductor in the equilibrium regime [25, 27].

The study of E_k has been useful to reveal the vortex dynamics of the superconducting condensate in different high temperature superconducting cuprates (HTSC) [27, 28, 29, 30]. Here we show how the analysis of E_k can also let us to indirectly investigate the nuances of the DOS at Fermi level and thus to obtain information on the pseudogap phenomenon from the inside of the superconducting phase. From this analysis we find that, in the underdoped regime, the amplitude of E_k at fixed field and reduced temperature T/T_c decreases steadily with decreasing holes density, consistently with expectations for a decreasing DOS at the Fermi level in that regime. Going further, E_k goes through a sharp maximum at $p \sim 0.18$, in the

slightly overdoped regime. We ascribe this peak to a van Hove singularity related to the sudden closing of the pseudogap phase occurring at this carriers density. This result is in accordance with the scenario where the pseudogap is related to excitations different from those giving origin to the superconducting state. Finally, fittings of the ratio $E_k/(\mu_0 H)$ to $(\mu_0 H)$ let us to obtain the superfluid density ρ_s . When ρ_s is plotted as a function of the hole concentration, it reveals a deviation of the Uemura relation around the optimal doping. Consequently, the values of p where the critical temperature and the superfluid density are maximal do not coincide. We attribute the deviation of the Uemura's law to the presence of pseudogap phase.

2 Materials and Methods

Several $\text{Bi}_2\text{Sr}_2\text{CaCu}_2\text{O}_{8+\delta}$ single crystals were synthesized by the the auto-flux method following the procedure described in Ref. [31, 32]. The crystals have the form of platelets with size between 1 - 3 mm and thickness around 30 μm . The hole density of the as-grown crystals was modified by thermal treatments at fixed temperatures in vacuum or oxygen atmosphere to remove or add oxygen, respectively [31, 32]. The quality and uniqueness of the crystallographic phase was probed, for each sample, by X-rays diffraction measurements performed with a SIEMENS D5000 diffractometer equipped with a cooper anode. The obtained diffraction patterns showed only even and sharp (00l) peaks.

Zero field cooling (ZFC) and field cooling (FC) magnetization measurements were carried out in fields ranging from $\mu_0 H = 1$ mT up to $\mu_0 H = 500$ mT in the configuration where the field is applied parallel to the c -axis. A Quantum Design XL5-MPMS SQUID magnetometer was used in these experiments. The critical temperatures reported here for all samples were extracted from the ZFC curves at $\mu_0 H = 1$ mT; $T_c(H)$ was estimated as the intersection point of two straight lines fitted to the data in the normal and superconducting phases; this procedure is exemplified in the inset of Fig. 1 for a different applied field ($\mu_0 H = 0.5$ T). The irreversibility temperature T_{irr} was also obtained from each pair of ZFC and FC magnetizations. This characteristic temperature is the lowest limit of the temperature range where the equilibrium magnetization is straightforwardly obtained from the data. The irreversibility temperature for each value of magnetic field was defined by the point where the difference between the FC and ZFC magnetizations becomes immeasurably small. The locus of T_{irr} for a fixed magnetic field $\mu_0 H = 500$ mT is exemplified in the main frame of Fig. 1.

The experimental magnetization between T_{irr} and T_c was used for obtaining the kinetic energy density with the help of Eq. 1, as will be shown in the next section. The corresponding magnetic induction was

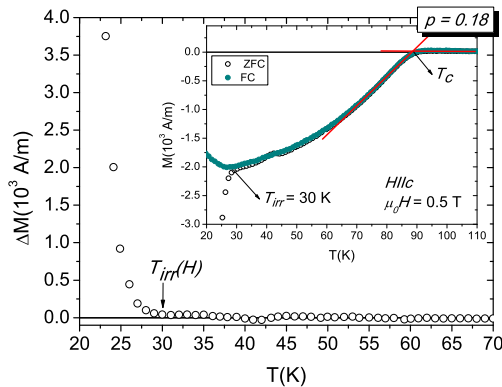


Figure 1: Representative curve of the difference between the zero field cooled (ZFC) and field cooled (FC) magnetic moments ($\Delta M = M_{FC} - M_{ZFC}$) for a Bi-2212 sample in the optimally doped regime. T_{irr} is the temperature where this difference becomes larger than zero. The inset shows graphically the criterion used for determining T_c at each value of applied magnetic field. There the T_{irr} is also shown as the temperature where the ZFC and FC curves split apart.

calculated as

$$B = \mu_0[H_{ap} - (1 - \eta)M], \quad (2)$$

where μ_0 is the vacuum permeability, H_{ap} is the applied field in A/m, M is the magnetization and η is the geometric demagnetization factor. This factor was estimated with basis on the calculations presented in Ref. [33] and by approximating the samples' shape by ellipsoids. The hole concentrations p were calculated using the quadratic, empirical relation [10]:

$$T_c = T_{c,max}[1 - 82.6(p - 0.16)^2]. \quad (3)$$

The superconducting dome as obtained from the $T_c(p)$ data for our samples and from fittings to Eq. (3) is shown in Fig. 2.

3 Results and discussion

Figure 3 shows the calculated E_k as a function of the reduced temperature (T/T_c) for a constant magnetic field $\mu_0 H = 500$ mT. One observes that E_k extrapolates to zero at the critical temperature in all cases. At most, weak rounding effects due to thermal fluctuations are perceived in the close vicinity of T_c . Previous studies in optimally and underdoped samples of YBCO (YBCO) [28], optimally doped Bi-2212 [28] and $\text{La}_{1.9}\text{Sr}_{0.1}\text{CuO}_4$ [34], reported that an appreciable amount of E_k subsists above T_c . The kinetic energy

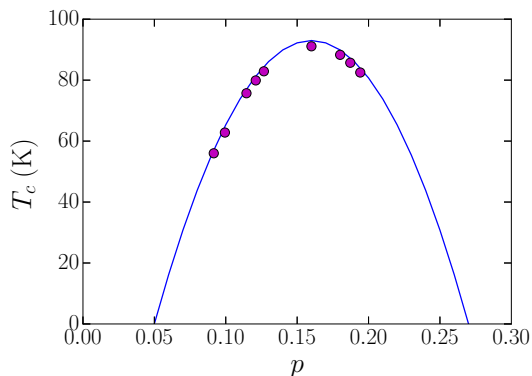


Figure 2: Superconducting critical temperature obtained from magnetization curves measured at $\mu_0 H = 1$ mT as a function of the hole doping for all the samples studied in this work (points). Error bars are within the size of the symbols. The continuous line is a fitting to Eq. (3).

excess found by authors in Refs. [28] and [34] was interpreted by them as resulting from non-correlated Cooper pairs characterizing the pseudogap phase. Results in Fig. 3, however, are rather indicating that the dependence of E_k with field and temperature is mostly related to the superconducting gap, as expected with basis on the BCS theory. We note that the observation of a certain E_k amplitude above T_c can be alternatively explained as an effect of strong thermal fluctuations.

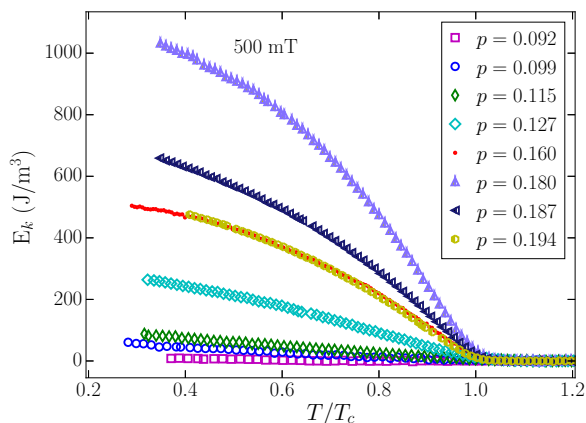


Figure 3: Kinetic energy density in a constant field $\mu_0 H = 500$ mT as a function of the normalized temperature for Bi-2212 crystals with the quoted carrier concentrations. The highest kinetic energy density is observed for the sample with $p = 0.180$ (see Fig. 4)

We plot in Fig. 4 the amplitude of E_k measured for each sample at $T = 0.8T_c$ and $\mu_0 H = 500$ mT as a function of the holes density p . A prominent feature in Fig. 4 is the sharp maximum of E_k that occurs at $p = 0.18$. This value for p does not match with the one where the maximal critical temperature is observed

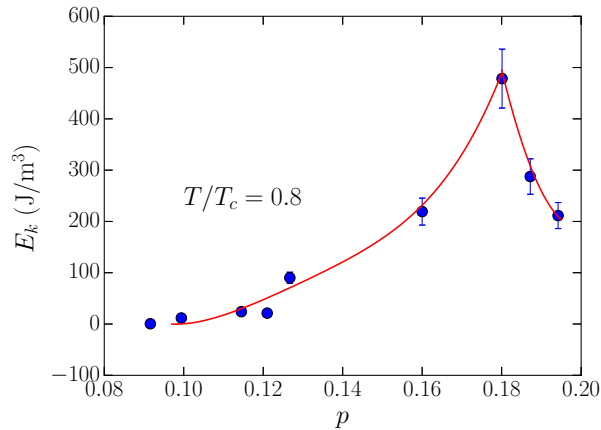


Figure 4: Amplitude of the kinetic energy density at the reduced temperature $T/T_c = 0.8$ as a function of the holes concentration. The continuous line is a guide for the eyes.

($p = 0.16$). Moreover, the E_k vs. p curve does not follow the same dome-like shape of the T_c vs. p curve, as expected from the Uemura relation. Then, the observed peak in E_k suggests that some unusual variation of the properties ruling the kinetic energy density in the superconducting state of Bi-2212 must be taken into account.

The superconducting gap, identified in Angle Resolved Photo-emission Spectroscopy (ARPES) around the nodal region of the Brillouin zone of Bi-2212, is nearly independent of the carrier concentration in the underdoped region of the dome-like phase diagram [9, 11, 35]. Assuming the validity of this observation, we infer that the dependence of the measured kinetic energy density with the carriers concentration shown in Fig. 4 does not follow the superconducting gap and might be at least partially attributed to some different phenomenon. On the other hand, the results in Fig. 3 suggest that the temperature and magnetic-field dependences of E_k are mainly ruled by the superconducting order parameter, as expected. Thus, the behavior of $E_k(H, T, p)$ in our Bi-2212 samples suggests that some distinct electronic phase coexists with the superconducting state below T_c .

Motivated by the possibility of obtaining further insight on the validity of the above outlined interpretation, we analyze in detail the behavior of E_k as a function of the magnetic field. As in Ref. [29], we assume that the magnetization of our samples is well described by the London approximation to the GL theory; this approximation is valid in the low field region where vortices do not overlap significantly. Then, the London equation for \mathbf{M} was used to obtain \mathbf{B} , and both were replaced in Eq. (1) which remains valid within this

context [25, 27]. We deduce the following expression for E_k [29]:

$$\frac{E_K(\mu_0 H)}{\mu_0 H} = \frac{\phi_0}{8\pi\lambda^2\mu_0} \ln \frac{\beta_L \mu_0 H_{c2}}{\mu_0 H} - \left(\frac{\phi_0}{8\pi\lambda^2} \right)^2 \frac{1}{\mu_0^2 H} \left(\ln \frac{\beta_L \mu_0 H_{c2}}{\mu_0 H} \right)^2, \quad (4)$$

where ϕ_0 is the magnetic flux quantum, μ_0 is the vacuum permeability, λ is the London penetration depth, H is the applied field, H_{c2} is the upper critical field, and β_L is a geometrical parameter of order unity.

Fittings of the experimental points to Eq. (4) were performed by using a PYTHON program to extract both the higher critical field and the penetration depth for each sample at some fixed temperatures. The fitting results are presented as solid lines in Fig. 5(a) which is for a reduced temperature $T/T_c = 0.8$ for all samples. The fitting parameters for this case are displayed in Table 1.

Table 1: Fitting parameters of the experimental points to Eq. (4) for all samples at $T/T_c = 0.8$.

p (± 0.001)	T_c (± 0.5) K	λ (± 0.05) μm	H_{c2} (± 0.5) mT
0.092	56.0	7.85	11.7
0.099	62.8	2.90	9.8
0.115	75.7	2.22	15.8
0.121	79.9	2.56	23.4
0.127	82.9	1.20	34.8
0.160	92.3	0.57	0.54
0.180	88.3	0.52	22.3
0.187	85.7	0.69	24.8
0.194	82.5	0.80	41.9

These extracted values for λ were used to calculate the superfluid density from [36]:

$$\rho_s = \frac{m}{2\mu_0 e^2} \frac{1}{\lambda^2}. \quad (5)$$

We plot in the main panel of Fig. 5(b) the superfluid density as a function of the hole concentration for the fixed reduced temperatures $T/T_c = 0.8$ (rounded symbols) and $T/T_c = 0.9$ (diamond symbols). As we are mostly interested in the overall qualitative behavior than in the numerical values of ρ_s , we assume $m/(2\mu_0 e^2) = 1$. The result in Fig. 5(b) is very similar to that found from ARPES measurements in Ref. [37] and basically reproduces the behavior of E_k as a function of p shown in Fig. 4. Though interesting, the similitude between results in Figs. 4 and 5(b) is not really surprising within the GL theory context. There, the relation $E_k \propto \langle |\psi|^2 \rangle$, where ψ is the superconducting order parameter and $\langle \dots \rangle$ symbolizes a spatial average [28], is satisfied. Consequently, the proportionality between the density of superconducting pairs,

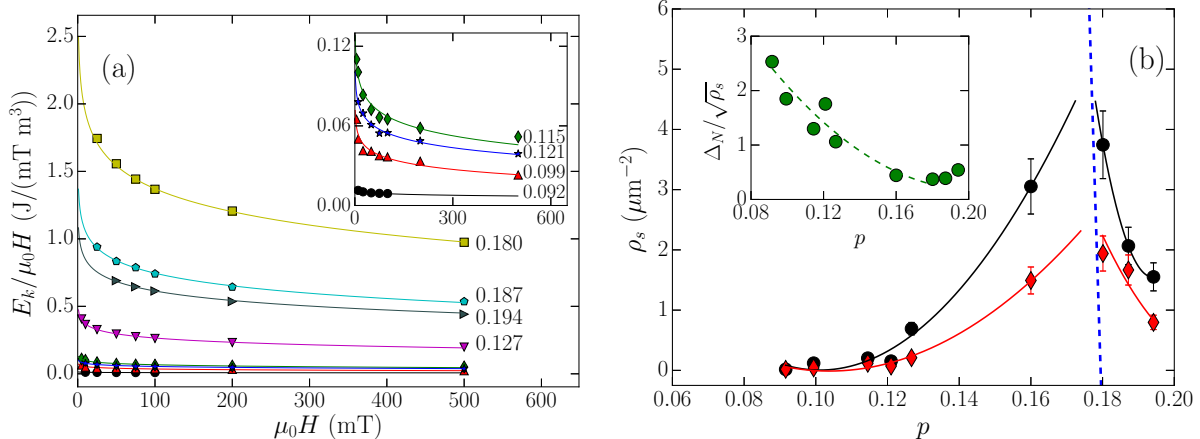


Figure 5: (a) $E_k/(\mu_0 H)$ vs. $\mu_0 H$ for most of the studied samples (p values are indicated for each curve); symbols represent the experimental points and continuous lines are fittings to Eq. 4. (b) Superfluid density $\rho_s = (1/\lambda^2)$ as a function of the holes concentration for $T/T_c = 0.8$ (rounded symbols) and $T/T_c = 0.9$ (diamond symbols). The continuous lines are guides for the eyes. The straight dashed line shows that the maximum of the ρ_s vs. p curves extrapolates to $p \sim 0.18$. In the inset of panel (b) the ratio between the superconducting gap and the square root of the superfluid density as calculated from Eq. 6 is represented as a function of p for $T/T_c = 0.9$ (see text). The dashed line is a guide for the eyes.

$|\psi|^2$, and λ^{-2} is expected. Finally, the comparison of Figs. 2 and 5(b) lets one to perceive that, as mentioned in the introduction, the series of Bi-2212 single crystal samples studied here violates the phenomenological Uemura's law which foresees a linear relation between ρ_s and T_c . In the underdoped regime, the graph ρ_s vs. T_c has a sub-linear behavior (not shown), qualitatively similar to that of the ρ_s vs. p in Fig. 5(b). The violation of the Uemura's law nearby the optimal doping had already been reported by C. C. Homes *et. al.* in Ref. [38], where the proportionality $\rho_s \propto \sigma_{dc} T_c$ (σ_{dc} is the conductivity measured near T_c) was proposed as the appropriate scaling to substitute the Uemura relation in all families of superconducting cuprates. On the other hand, as a further exemple of violation of the Uemura relation, J. Hetel *et. al.* [39] found a sublinear relation between T_c and the superfluid density in the strongly underdoped region of thick YBCO films.

The superfluid density ρ_s may be conceived as a measure of the toughness of the superconducting state against an external magnetic field. As the condensation energy is proportional to the critical field, tougher superconducting states have higher condensation energies and superfluid densities. In this sense, it is remarkable that the maximum of the ρ_s vs. p curves extrapolates to $p \sim 0.18$, as indicated by the straight, dashed line in the main panel of Fig. 5 (b)). This is consistent with results of thermodynamic measurements that show a steep increase of the condensation energy at $p \sim 0.19$ in $\text{Y}_{0.8}\text{Ca}_{0.2}\text{Ba}_2\text{Cu}_3\text{O}_{7-\delta}$ [11]. Additionally, the direct proportionality between E_k and ρ_s lead us to straightforwardly conclude that the doping depen-

dence of both of these quantities indicates that a sharp increase in the density of superconducting carriers occurs at $p = 0.18$. This conclusion agrees with the fact that, this same maximum is also present in the DOS of other HTSC systems, as estimated in Ref. [40] with basis on experimental results. The qualitative coincidences in the behavior of the kinetic energy density, entropy [37], superfluid density [36], and DOS [40] with respect to p in the Bi-2212 and other HTSC is indeed remarkable. All these results are compatible with the existence of a van Hove singularity (vHs) in the slightly overdoped region of the Bi-2212 phase diagram. Such singularity has been related to the steep ending of the pseudogap phase [9, 37] occurring simultaneously with a Lifshitz quantum phase transition where the active hole-like Fermi surface becomes electron-like [41, 42]. This is accompanied by a notable transition in k -space topology within the narrow range $p \sim 0.19 \pm 0.1$ [41]. Within this frame, the peak observed at $p \sim 0.18$ in our E_k vs. p and ρ_s vs. p curves suggests that, differently from T_c , the kinetic energy density and the superfluid density are rather related to the pseudogap energy scale.

It was found experimentally that in Bi-2212 the pseudogap energy (Δ^*) satisfies the relation [13]:

$$\Delta^* \propto \frac{\Delta_N}{\sqrt{\rho_s}}, \quad (6)$$

where $\Delta_N = 4.25k_B T_c$ [13] is the superconducting (nodal) gap. The quotient $\Delta_N/\sqrt{\rho_s}$ estimated from our data is presented as a function of p in the inset of Fig. 5 (b). Assuming the validity of Eq. (6), we interpret the minimum of $\Delta_N/\sqrt{\rho_s}$ observed at $p = 0.18$ as a consequence of a minimum in the pseudogap energy. This interpretation is consistent with our previous statement on the existence of a maximum in the density of superconducting carriers at the same p value. As mentioned before, that maximum is consequence of a Lifshitz transition apparently driven by the reduction of the strength of the electronic correlations with doping [43]. Thus, our results indicate that the reinforcement of the superfluid and kinetic energy densities in the superconducting state is related to the undermining of the excitations that give origin to the pseudogap phenomenon.

Our kinetic energy density results indirectly support the existence of a QCP by $p = 0.18$, in the lightly overdoped region of the Bi-2212 phase diagram; even so, these results don't rule out the possibility of the occurrence of the pseudogap in samples with $p \gtrsim 0.19$ in temperatures outside the superconducting dome. In fact, effects of the pseudogap up to $p \sim 0.22$ were observed in ARPES [9, 44] and high-field NMR [45] measurements performed on samples of the $\text{Bi}_2\text{Sr}_2\text{CuO}$ (Bi-2201) and Bi-2212 systems. In Refs. [9] and [44] the effects of pseudogap were observed up to $p \sim 0.22$ in temperatures above T_c ; there, the

authors put forward a phase diagram where the pseudogap goes into the superconducting dome drawing a positive-slope line starting at $p \sim 0.22$ and ending in a QCP at $p \sim 0.19$ over the horizontal axis. In Ref. [45] ultra-high magnetic fields were used to suppress the superconductivity to barely observe the pseudogap phenomenon. Our results show that the temperature-dependence of E_k is dominated by the superconducting order parameter, while its doping-dependence is rather dominated by the pseudogap. All these scenarios are consistent with a picture where the superconducting and pseudogap phases coexist, but they compete at the point that for samples with $p > 0.19$ the pseudogap is no longer able to manifest itself overwhelmingly inside the superconducting dome. To finish this point, the fact that our results support the location of the QCP nearer, and even a little lower than $p \sim 0.19$ may be due to the fact that we are approaching the pseudogap from the point of view of an intrinsically superconducting parameter in which the pseudogap is already manifesting more weakly.

Another possible evidence of competition among different electronic states in Bi-2212 comes from a study of the normal-phase susceptibility in the same set of samples investigated in the present work [31]. Those results showed that a maximum in the DOS occurs at $p \sim 0.16$ and not at $p \sim 0.18$. The discrepancy between these two characteristic values for p is probably consequence of the used experimental techniques. Depending on the temperature range where these methods are implemented, some are more sensitive to the effects related to the nodal region of the Brillouin zone, others to the antinodal region.

4 Conclusion

We studied the overall behavior of the in-field kinetic energy density in a series of Bi-2212 single crystals with different carrier density. Results of E_k as a function of the temperature, doping and magnetic field were analyzed with the aim of identifying features related to the pseudogap phenomenon. From the E_k vs. T curves, we conclude that the field-induced kinetic energy changes with temperature similarly to the superconducting order parameter. At fixed temperature and variable fields, E_k is quite well described by the London approximation to the GL theory. On the other hand, the variation of E_k with doping can not be explained solely with basis on the superconducting order parameter. In samples with $p < 0.18$, both the kinetic energy and superfluid densities are strongly depressed. This behavior is expected in properties which are closely dependent on the pseudogap. A sharp maximum is observed in E_k at the carrier concentration $p = 0.18$ (also evident in the superfluid density). This particular feature is consistent with the occurrence of a van Hove singularity in the DOS coincident with the suppression of the pseudogap.

The fact that E_k is ruled by both the superconducting and pseudogap energy scales strongly suggests that the superconducting state and the pseudogap phenomenon coexist inside the superconducting dome for all Bi-2212 samples with $p \leq 0.18$. This general conclusion is consistent with a model that attributes essentially different origins for the superconducting state and the pseudogap phenomenon. A comparison between our results and other experimental data with theoretical analyses lead us to conclude that the pseudogap phenomenon influences the behavior of some quantities intrinsically related to superconductivity in the HTSC. Consequently, one may expect that its effects also occur inside the superconducting dome.

Acknowledgments

This work was partially financed by the Brazilian agencies FAPERGS and CNPq (Grant PRONEX 16/0490-0). L. F. Lopes benefits from a CNPq fellowship. J. P. Peña received a post-doctoral fellowship of the Brazilian Agency CAPES.

References

- [1] A. A. Kordyuk, *Low Temp. Phys.* 41, 319 (2015)
- [2] I. M. Vishik, *Rep. Prog. Phys.* 81, 062501 (2018)
- [3] J. W. Loram, K. A. Mirza, J. R. Cooper, W.Y. Liang, *Phys. Rev. Lett.* 71, 1740 (1993)
- [4] J. W. Loram, J. Luo, J. R. Cooper, W. Y. Liang, J. L. Tallon, *J. Phys. Chem. Solids* 62, 59 (2001)
- [5] W. Warren Jr., R. E. Walstedt, G. F. Brennert, R. J. Cava, R. Tycko, R. F. Bell, and G. Dabbagh, *Phys. Rev. Lett.* 62, 1193 (1989)
- [6] C. Renner, B. Revaz, J. Y. Genoud, K. Kadowaki, and O. Fischer, *Phys. Rev. Lett.* 80, 149 (1998)
- [7] H. Ding, T. Yokoya, J. C. Campuzano, T. Takahashi, M. Randeria, M. R. Norman, T. Mochiku, K. Kadowaki, and J. Giapintzakis, *Nature* 382, 51 (1996)
- [8] S. Tajima, *Rep. Prog. Phys.* 79, 094001 (2016)
- [9] M. Hashimoto, I. M. Vishik, Rui-Hua He, T. P. Devereaux, and Zhi-Xun Shen, *Nat. Phys.* 10, 483 (2014)

- [10] J. L. Tallon, C. Bernhard, H. Shaked, R. L. Hitterman, and J. D. Jorgensen, *Phys. Rev. B* 51, 12911 (1995)
- [11] J. L. Tallon, and J. W. Loram, *Physica C* 349, 53 (2001)
- [12] S. H. Naquib, and R. H. Islam, *Supercond. Sci. Technol.* 21, 105017 (2008)
- [13] H. Anzai, A. Ino, M. Arita, H. Namatame, M. Taniguchi, M. Ishikado, K. Fujita, S. Ishida, and S. Uchida, *Nat. Comm.* 4, 1815 (2013)
- [14] Tigran A. Sedrakyan, and A. V. Chubukov, *Phys. Rev. B* 81, 174536 (2010)
- [15] M. Charlebois, S. Verret, A. Foley, O. Simard, D. Senechal, and A. M. S. Tremblay, *Phys. Rev. B* 96, 205132 (2017)
- [16] Ching-Kit Chan and Tai-Kai Ng, *Phys. Rev. B* 74, 172503 (2006)
- [17] Tai-Kai Ng, *Europhysics letters* 82(4), 47004 (2008)
- [18] Y. Sato, S. Kasahara, H. Murayama, Y. Kasahara, E. G. Moon, T. Nishizaki, T. Loew, J. Porras, B. Keimer, T. Shibauchi, and Y. Matsuda, *Nat. Phys.* 13, 1074 (2017)
- [19] L. Zhao, C. A. Belvin, R. Liang, D. A. Bonn, W. N. Hardy, N. P. Armitage, and D. Hsieh, *Nat. Phys.* 13, 250 (2017)
- [20] J. Zhang, Z. Ding, C. Tan, K. Huang, O. O. Bernal, Pei-Chun Ho, G. D. Morris, A. D. Hillier, P. K. Biswas, S. P. Cottrell, H. Xiang, X. Yao, D. E. MacLaughlin, and Lei Shu, *Science Advances* 4 (1), eaao5235 (2018)
- [21] L. Chaix, G. Ghiringhelli, Y. Y. Peng, M. Hashimoto, B. Moritz, K. Kummer, N. B. Brookes, Y. He, S. Chen, S. Ishida, Y. Yoshida, H. Eisaki, M. Salluzzo, L. Braicovich, Z.-X. Shen, T. P. Devereaux, and W. S. Lee, *Nat. Phys.* 13, 952 (2017)
- [22] S. Badoux, W. Tabis, F. Laliberte, G. Grissonnanche, B. Vignolle, D. Vignolles, J. Beard, D. A. Bonn, W. N. Hardy, R. Liang, N. Doiron-Leyraud, L. Taillefer and C. Proust, *Nature* 531, 210 (2016)
- [23] S. E. Sebastian, N. Harrison, F. F. Balakirev, M. M. Altarawneh, P. A. Goddard, Ruixing Liang, D. A. Bonn, W. N. Hardy, and G. G. Lonzarich, *Nature* 511, 61 (2014)

- [24] A. Shekhter, J. Ramshaw, R. Liang, W. N. Hardy, D. A. Bonn, Fedor F. Balakirev, R. D. McDonald, J. B. Betts, S. C. Riggs, and A. Migliori, *Nature* 498, 75 (2013)
- [25] M. M. Doria. *J. Supercond. Nov. Mag.* 22, 235–238 (2009)
- [26] M.M. Doria, J. E. Gubernatis, D. Rainer, *Phys. Rev. B* 39, 9573 (1989)
- [27] M. M. Doria, S. Salem-Sughi Jr., I.G. de Oliveira, L. Ghivelder, and E.H. Brandt, *Phys. Rev. B* 65, 144509 (2002)
- [28] S. Salem-Sugui Jr., M. M. Doria, A.D. Alvarenga, V. N. Vieira, P. F. Farinas, J.P. Sinnecker, *Phys. Rev. B* 76, 132502 (2007)
- [29] J. P. Peña · D. B. Martínez · C. A. Parra Vargas · A. G. Cunha · J. L. Pimentel Jr. · P. Pureur, *Braz J Phys* 43, 22–27 (2013)
- [30] V. N. Vieira, A. P. A. Mendonça, F. T. Dias, M. L. Hneda, P. Pureur, J. Schaf, and F. Mesquita, *J. Phys.Conf. Series* 592, 012062 (2015)
- [31] L. F. Lopes, J. P. Peña, J. Schaf, M. A. Tumelero, V. N. Vieira, P. Pureur, *Physica B* 536, 855 - 859 (2018)
- [32] L. F. Lopes, S. T. Jaeckel, V. N. Vieira, R. F. Lopes, A. M. Turatti, J. L. Pimentel, J. Schaf, P. Pureur, To be published-*Materials Today* (2019)
- [33] J. A. Osborn, *Phys. Rev.* 67, 351 (1945)
- [34] M.M. Doria, S. Salem-Sugui Jr. *Phys. Rev. B* 78, 134527 (2008)
- [35] K. Tanaka, W. S. Lee , D. H. Lu, A. Fujimori, T. Fujii, Risdiana, I. Terasaki, D. J. Scalapino, T. P. Devereaux, Z. Hussain, Z. X. Shen, *Science* 314, 1910 - 1914 (2006)
- [36] J. L. Tallon, J. W. Loram, J. R. Cooper, C. Panagopoulos, and C. Bernhard, *Phys. Rev. B* 68, 180501(R) (2003)
- [37] J. G. Storey, J. L. Tallon, and G. V. M. Williams, *Phys. Rev. B* 77, 052504 (2008)
- [38] C. C. Homes, S. V. Dordevic, M. Strongin, D. A. Bonn, R. Liang, W. N. Hardy, S. Komiya, Y. Ando, G.Yu, N. Kaneko, X. Zhao, M. Greven, D. N. Basov, T. Timusk, *Nature* 430, 539 (2004)

- [39] I. Hetel, T. R. Lemberger, and M. Randeria, *Nat. Phys.* 3, 700 (2007)
- [40] J. G. Storey, J. L. Tallon, and G. V. M. Williams, *Phys. Rev. B* 76, 174522 (2007)
- [41] K. Fujita, C. K. Kim, I. Lee, J. Lee, M. H. Hamidian, I. A. Firmo, S. Mukhopadhyay, H. Eisaki, S. Uchida, M. J. Lawler, E. A. Kim, J. C. Davis, *Science* 344, 612 (2014)
- [42] S. Benhabib, A. Sacuto, M. Civelli, I. Paul, M. Cazayous, Y. Gallais, M.-A. Méasson, R. D. Zhong, J. Schneeloch, G. D. Gu, D. Colson, and A. Forget, *Phys. Rev. Lett.* 114, 147001 (2015)
- [43] H. Bragança, S. Sakai, M. C. O. Aguiar, and M. Civelli, *Phys. Rev. Lett.* 120, 067002 (2018)
- [44] M. Hashimoto *et. al.*, *Nat. Mat.* 14, 37 - 42 (2014)
- [45] S. Kawasaki, C. Lin, P. L. Kuhns, A. P. Reyes, and Guo-qing Zheng, *Phys. Rev. Lett.* 105, 137002 (2010)